

Heavy quark production via leptoquarks at a neutrino factory

Ashok Goyal* and Poonam Mehta†

Department of Physics & Astrophysics, University of Delhi, Delhi 110 007, India

Sukanta Dutta‡

Physics Department, SGTB Khalsa College, University of Delhi, Delhi 110 007, India

(Received 2 December 2002; published 31 March 2003)

The proposed neutrino factory based on a muon storage ring (MSR) is an ideal place to look for heavy quark production via neutral current and charged current interactions. In this article, we address the issue of contributions coming from mediating leptoquarks (LQs) in $\nu_\mu(\bar{\nu}_e)$ - N scattering, leading to the production of $b(\bar{b})$ at a MSR, and investigate the region where LQ interactions are significant in the near-site experiments.

DOI: 10.1103/PhysRevD.67.053006

PACS number(s): 14.60.Pq, 13.15.+g, 14.65.Fy

I. INTRODUCTION

It is widely believed that the proposed neutrino factory (NF) based on a muon storage ring (MSR) capable of supplying a well calibrated and intense beam of roughly $\approx 10^{20}\nu_\mu(\bar{\nu}_\mu)$ and $\bar{\nu}_e(\nu_e)$ per year through 50 GeV muon decays will open up an unprecedented opportunity to reveal the world of neutrinos and to provide a physical laboratory for testing physics beyond the standard model (SM) [1,2]. Recent strong indications of atmospheric neutrino oscillations ($\nu_\mu \rightarrow \nu_x$, where x is not e) [3] have rekindled interest in accelerator experiments that could study the same range of parameter space. The solar neutrino deficit is interpreted either as matter enhanced Mikheyev-Smirnov-Wolfenstein oscillations [4] or as vacuum oscillations [5] that deplete the original ν_e 's, presumably in favor of ν_μ 's. The role of a NF in determining the masses and mixing angles for $\nu_\mu \leftrightarrow \nu_\tau$ and $\bar{\nu}_e \leftrightarrow \bar{\nu}_\mu$ oscillations, both at short and long baseline experiments, has been extensively discussed in the literature. The investigation of physics beyond the SM through certain novel interactions in the neutrino sector, in particular, the appearance of τ and wrong sign μ signals in new physics scenarios, such supersymmetric (SUSY) theories with broken R parity [6] and theories that allow leptoquark (LQ) mediated lepton flavor violating (LFV) interactions [7], have been dealt with in our earlier works [6,7]. With the same motivation to look for the role played by the nonstandard interactions at a NF, the production of heavy quarks through ν_μ - N scattering in an R -parity violating SUSY theory was investigated recently [8] and it was shown that it is possible to have significant event rates for $b(\bar{b})$ production via both neutral current (NC) and charged current (CC) interactions. We should emphasize here that in SM the production of $b(\bar{b})$ is severely suppressed at tree level. Thus a considerable number of $b(\bar{b})$ or an excess well above the SM rate at a NF would unequivocally imply the existence of nonstandard

physics in the neutrino sector. In contrast to SM, b quark production via nonstandard ν - N scattering processes can take place at the tree level itself via the CC interactions, $\nu_\mu \bar{u} \rightarrow \mu^- \bar{b}$, $\nu_\mu \bar{c} \rightarrow \mu^- \bar{b}$, and $\bar{\nu}_e u \rightarrow e^+ b$, all of which are suppressed in the SM either due to the Cabibbo-Kobayashi-Maskawa (CKM) matrix elements V_{ub} or due to the interaction of ν_μ with sea quarks present inside the nucleon. The corresponding NC processes $\nu_\mu d \rightarrow \nu_\mu b$ and $\bar{\nu}_e d \rightarrow \bar{\nu}_e b$ can occur only at one loop level in the SM.

In this context, it is worthwhile to consider theories with leptoquarks which occur naturally in grand unified theories, superstring inspired E_6 models and in Technicolor models, [9] and study heavy flavor (b, \bar{b}) production in scattering of neutrinos on a fixed isonucleon target with LQs as mediators of the interaction. In our earlier work, we have studied the contribution of mediating lepton flavor violating LQs in $\nu_\mu(\bar{\nu}_e)$ N scattering, leading to an enhanced production of τ 's and wrong sign μ 's at MSR, and investigated the region where LQ interactions are significant in the near-site and short baseline experiments, and we found that *one can constrain LFV couplings between the first and third generation, the bounds on which are not generally available*. With the same spirit in this present work, we investigate the b quark production in both NC and CC channels through $\nu_\mu(\bar{\nu}_e)$ N scattering at the NF, mediated by scalar and vector leptoquarks. It is worth mentioning that we consider the $\bar{\nu}_e$ beam also for production of b, \bar{b} in both the NC and CC channels unlike Ref. [8]. For the present case, since we are interested in new physics effects alone and not the oscillation effects, it is desirable to confine ourselves to near-site experiments where the neutrino detectors are placed at a very short distance (typically 40 m) from the storage ring. Here we do not consider the LFV processes. The processes that we consider in this article for the b, \bar{b} production via NC and CC channels are

$$\text{NC: } \nu_\mu d \rightarrow \nu_\mu b, \quad \bar{\nu}_e d \rightarrow \bar{\nu}_e b; \quad (1)$$

$$\text{CC: } \nu_\mu \bar{u} \rightarrow \mu^- \bar{b}, \quad \bar{\nu}_e u \rightarrow e^+ b. \quad (2)$$

*Email address: agoyal@ducoss.ernet.in

†Email address: pmehta@physics.du.ac.in; mpoonam@mri.ernet.in

‡Email address: Sukanta.Dutta@cern.ch

The total number of b, \bar{b} quark production events per year via either CC or NC interactions can be written as

$$\mathcal{N}_{b, \bar{b}} = \mathcal{N}_n \int \frac{d^2 \sigma_{NC/CC}^{\nu, \bar{\nu}}}{dx dy} \left[\frac{dN_{\nu, \bar{\nu}}}{dE_{\nu_i, \bar{\nu}_i}} \right] \mathcal{P}_{surv}[\nu_i(\bar{\nu}_i) \rightarrow \nu_i(\bar{\nu}_i)] dE_{\nu_i(\bar{\nu}_i)} q(x) dx dy, \quad (3)$$

where \mathcal{N}_n is the number of nucleons per kT of the target material,¹ x and y are the Bjorken scaling variables, q and q' are the quarks in the initial and final states, respectively, and $q(x)$ is the quark distribution function. The differential parton level cross section can be expressed as

$$\frac{d^2 \sigma_{NC/CC}^{\nu, \bar{\nu}}}{dx dy} = \left[\frac{d^2 \sigma_{NC/CC}^{\nu, \bar{\nu}}}{dx' dy'} \right] \frac{\partial(x', y')}{\partial(x, y)} = \left[\frac{|\mathcal{M}(x', y')|_{NC/CC}^2}{32\pi \hat{S}} \right], \quad (4)$$

where $y' = -\hat{t}/\hat{S} = Q^2/(2ME_{\nu} x')$ and x' is the *slow rescaling* variable² that arises due to the mass shell constraint of the heavy quark produced in the final state,

$$x' = \frac{Q^2 + m_Q^2}{2M\nu} = x + \frac{m_Q^2}{2ME_{\nu} y}.$$

Therefore

$$\frac{\partial(x', y')}{\partial(x, y)} = 1, \quad (5)$$

M being the nucleon mass, E_{ν} being the neutrino energy, and $\nu = E_{\nu_i} - E_{l^-} (E_{\nu_i}^- - E_{l^+})$. \hat{S} is the parton level c.m. energy and $[dN_{\nu, \bar{\nu}}/dE_{\nu_i, \bar{\nu}_i}]$ is the differential ν ($\bar{\nu}$) flux. The survival probability of a particular neutrino flavor (i) is given by $\mathcal{P}_{surv}(\nu_i \rightarrow \nu_i) = 1 - \mathcal{P}_{osc}(\nu_i \rightarrow \nu_j)$ where j takes all possible values: $j = e, \mu, \tau$ but $j \neq i$.³

The effective Lagrangian with the most general dimensionless, $SU(3)_c \times SU(2)_L \times U(1)_Y$ invariant couplings of *scalar* and *vector* LQs satisfying baryon (B) and lepton number (L) conservation [suppressing color, weak isospin, and generation (flavor) indices] is given [10] by

$$\mathcal{L} = \mathcal{L}_{|F|=2} + \mathcal{L}_{|F|=0},$$

where

¹ $\mathcal{N}_n = 6.023 \times 10^{32}$ for a target of mass 1 kT.

²For production of a heavy quark from a light quark, the heavy quark mass modifies the scaling variable of the quark distribution. x' is the quark momentum fraction appropriate for absorbing the virtual W described by ν and Q^2 .

³For the two flavor oscillation case, $\mathcal{P}_{osc}(\nu_i \rightarrow \nu_j) = \sin^2 2\theta_m \sin^2(1.27 \Delta m^2 (\text{eV}^2) [L(\text{km})/E_{\nu} (\text{GeV})])$, where L is the baseline length, E_{ν} is the neutrino energy, Δm^2 is the mass-squared difference between the corresponding physical states, and θ_m is the mixing angle between flavors.

$$\begin{aligned} \mathcal{L}_{|F|=2} = & [g_{1L} \bar{q}_L^c i \tau_2 l_L + g_{1R} \bar{u}_R^c e_R] S_1 + \tilde{g}_{1R} \bar{d}_R^c e_R \tilde{S}_1 \\ & + g_{3L} \bar{q}_L^c i \tau_2 \tilde{\tau}_L \tilde{S}_3 + [g_{2L} \bar{d}_R^c \gamma^\mu l_L + g_{2R} \bar{q}_L^c \gamma^\mu e_R] V_{2\mu} \\ & + \tilde{g}_{2L} \bar{u}_R^c \gamma^\mu l_L \tilde{V}_{2\mu} + \text{c.c.}, \end{aligned}$$

$$\begin{aligned} \mathcal{L}_{|F|=0} = & [h_{2L} \bar{u}_R l_L + h_{2R} \bar{q}_L i \tau_2 e_R] R_2 + \tilde{h}_{2L} \bar{d}_R l_L \tilde{R}_2 \\ & + \tilde{h}_{1R} \bar{u}_R \gamma^\mu e_R \tilde{U}_{1\mu} + [h_{1L} \bar{q}_L \gamma^\mu l_L \\ & + h_{1R} \bar{d}_R \gamma^\mu e_R] U_{1\mu} + h_{3L} \bar{q}_L \tilde{\tau} \gamma^\mu l_L U_{3\mu} + \text{c.c.}, \end{aligned} \quad (6)$$

where q_L, l_L are the left-handed quarks and lepton doublets and e_R, d_R, u_R are the right-handed charged leptons, down-, and up-quark singlets, respectively. The scalar (i.e., S_1, \tilde{S}_1, S_3) and vector (i.e., V_2, \tilde{V}_2) LQs carry the fermion number $F = 3B + L = -2$, while the scalar (i.e., R_2, \tilde{R}_2) and vector (i.e., U_1, \tilde{U}_1, U_3) LQ have $F = 0$.

Numerous phenomenological studies have been made in order to derive bounds and put stringent constraints on LQ couplings, particularly from low energy flavor changing neutral current (FCNC) processes [11] that are generated by scalar and vector LQ interactions. Direct experimental searches for leptoquarks have also been carried out at the e - p collider and bounds obtained [11,12], and, in particular, bounds obtained from B meson decays ($B \rightarrow l^+ l^- X$, where $l^+ l^- = \mu^+ \mu^-, e^+ e^-$) and also bounds derived from meson-antimeson ($B\bar{B}$) mixing would have a direct bearing on the processes considered here. This is because the low energy limit puts a stringent bound on effective four-fermion interactions involving two leptons and two quarks, and since at the NF the center of mass energy in collision is low enough, we can consider the neutrino-quark interaction as an effective four-fermion interaction. The bounds on effective couplings used in this paper are the LQ couplings over the LQ mass squared and are derived on the assumption that the individual leptoquark coupling contribution to the branching ratio does not exceed the experimental upper limits and in the branching ratios only one leptoquark coupling is considered by switching off all the other couplings. All couplings are considered to be real, and combinations of left and right chirality coupling are not considered. This article is outlined as follows. We discuss the b (\bar{b}) production through ν ($\bar{\nu}$) N interactions via NC and CC channels in Secs. II and III, respectively, and give the plots of event rate versus muon beam energy. In Sec. IV we outline the conclusions drawn from our results.

II. b (\bar{b}) PRODUCTION VIA NC PROCESSES

Let us first consider the possible NC processes that can lead to b/\bar{b} in the final state. There is no SM tree level process in the NC channel as NC processes leading to b/\bar{b} can only occur at one loop level in the SM. However, there can be two possible nonstandard tree level NC processes that can lead to the production of b/\bar{b} in the final state, due to the

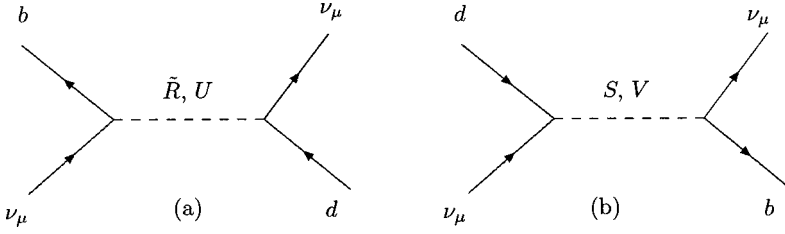


FIG. 1. b production via NC process ($\nu_\mu + d \rightarrow \nu_\mu + b$) from scalar and vector LQs: (a) u -channel process corresponding to $|F|=0$ LQs and (b) s -channel process corresponding to $|F|=2$ LQs.

presence of both ν and $\bar{\nu}$ of different flavors from μ decay, viz., $\mu^- \rightarrow e^- \nu_\mu \bar{\nu}_e$: (1) $\nu_\mu + d \rightarrow \nu_\mu + b$, (2) $\bar{\nu}_e + d \rightarrow \bar{\nu}_e + b$. For the two NC processes mentioned above, we have both s - and u -channel diagrams arising from the relevant interaction terms in the effective LQ Lagrangian. For the first process, $\nu_\mu + d \rightarrow \nu_\mu + b$ (shown in Fig. 1), there are two possible u -channel diagrams mediated by LQs ($\tilde{R}^\dagger, U^\dagger$) carrying $|F|=0$ and charge = $1/3$, while there are three possible s -channel diagrams that are mediated by LQs (S^\dagger, V^\dagger) carrying $|F|=2$ and charge = $-1/3$. For the second process, $\bar{\nu}_e + d \rightarrow \bar{\nu}_e + b$ (shown in Fig. 2), the two possible s -channel diagrams are mediated by LQs (\tilde{R}, U) carrying $|F|=0$ and charge = $-1/3$, while the three possible u -channel diagrams are mediated by LQs (S, V) carrying $|F|=2$ and charge = $1/3$.

We first consider the production of b from ν_μ (obtained from μ^- decay) interactions with nucleons via NC u -channel processes for the $|F|=0$ case [Fig. 1(a)] and NC s -channel processes for the $|F|=2$ case [Fig. 1(b)]. There are, in all, two diagrams contributing to production of b via $(\nu_\mu + d \rightarrow \nu_\mu + b)$ in the u channel [Fig. 1(a)], one mediated by the charge = $1/3$, scalar LQ ($\tilde{R}_2^{-1/2\dagger}$) carrying $T_3 = -1/2$ and the other one by a vector LQ ($U_{3\mu}^\dagger$) with $T_3 = -1$, where T_3 is the weak isospin. The matrix element squared for two diagrams contributing to the u -channel NC process is

$$\begin{aligned}
 & |\mathcal{M}_{LQ}^{u\text{-chann}}(\nu_\mu d \rightarrow \nu_\mu b)|^2 \\
 &= [\hat{u}(\hat{u} - m_b^2)] \left[\frac{|\tilde{h}_{2L}\tilde{h}_{2L}|^2}{(\hat{u} - M_{\tilde{R}_2^{-1/2}}^2)^2} \right] + [4\hat{s}(\hat{s} - m_b^2)] \\
 &\quad \times \left[\frac{|\sqrt{2}h_{3L}\sqrt{2}h_{3L}|^2}{(\hat{u} - M_{U_{3\mu}^-}^2)^2} \right], \quad (7)
 \end{aligned}$$

where the Mandelstam variables at the parton level are given by $\hat{s} = (p_{\nu_\mu} + p_d)^2$, $\hat{t} = [p_{\nu_\mu}(\text{initial}) - p_{\nu_\mu}(\text{final})]^2$, and $\hat{u} = (p_{\nu_\mu} - p_b)^2$, with p_i denoting the four-momentum of the i th particle.

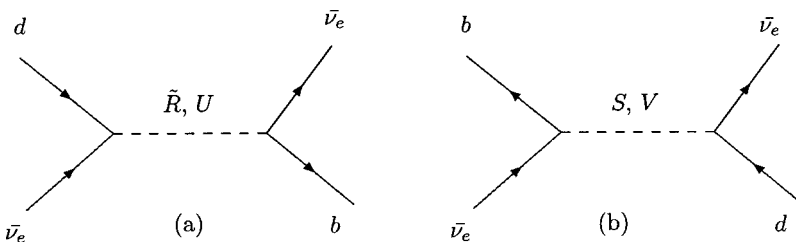


FIG. 2. b production via NC process ($\bar{\nu}_e + d \rightarrow \bar{\nu}_e + b$) from scalar and vector LQs: (a) s -channel process corresponding to $|F|=0$ LQs and (b) u -channel process corresponding to $|F|=2$ LQs.

In the s channel, two diagrams are mediated by charge = $-1/3$, scalar LQs ($S_1^\dagger, S_3^{0\dagger}$) with $T_3 = 0$, while one is mediated by a vector LQ ($V_{2\mu}^{-1/2\dagger}$) with $T_3 = -1/2$ [Fig. 1(b)]. The matrix element squared for all the three diagrams contributing to the NC s -channel process is

$$\begin{aligned}
 & |\mathcal{M}_{LQ}^{s\text{-chann}}(\nu_\mu d \rightarrow \nu_\mu b)|^2 \\
 &= [\hat{s}(\hat{s} - m_b^2)] \left[\frac{|g_{1L}g_{1L}|^2}{(\hat{s} - M_{S_1}^2)^2} + \frac{|g_{3L}g_{3L}|^2}{(\hat{s} - M_{S_3^0}^2)^2} \right. \\
 &\quad \left. + 2 \frac{|g_{1L}g_{3L}|^2}{(\hat{s} - M_{S_1}^2)(\hat{s} - M_{S_3^0}^2)} \right] + [4\hat{u}(\hat{u} - m_b^2)] \\
 &\quad \times \left[\frac{|g_{2L}g_{2L}|^2}{(\hat{s} - M_{V_{2\mu}^{-1/2}}^2)^2} \right]. \quad (8)
 \end{aligned}$$

Next we consider the production of b from $\bar{\nu}_e$ (also obtained from the μ^- decay) through interactions with nucleon via the NC s -channel process for the $|F|=0$ case [Fig. 2(a)] and NC u -channel process for the $|F|=2$ case [Fig. 2(b)]. There are, in all, two diagrams contributing to the production of b via $(\bar{\nu}_e + d \rightarrow \bar{\nu}_e + b)$ in the s channel [Fig. 2(a)], one mediated by the charge = $-1/3$, scalar LQ ($\tilde{R}_2^{-1/2}$) with $T_3 = -1/2$, while the other one is mediated by a vector LQ ($U_{3\mu}^-$) with $T_3 = -1$. The matrix element squared for the two diagrams contributing to the NC s -channel process is

$$\begin{aligned}
 & |\mathcal{M}_{LQ}^{s\text{-chann}}(\bar{\nu}_e d \rightarrow \bar{\nu}_e b)|^2 \\
 &= [\hat{s}(\hat{s} - m_b^2)] \left[\frac{|\tilde{h}_{2L}\tilde{h}_{2L}|^2}{(\hat{s} - M_{\tilde{R}_2^{-1/2}}^2)^2} \right] + [4\hat{u}(\hat{u} - m_b^2)] \\
 &\quad \times \left[\frac{|\sqrt{2}h_{3L}\sqrt{2}h_{3L}|^2}{(\hat{s} - M_{U_{3\mu}^-}^2)^2} \right], \quad (9)
 \end{aligned}$$

TABLE I. The best bounds on all relevant products of couplings (from B decays and $B\bar{B}$ mixing) taken from Table 15 of Ref. [11] by Davidson *et al.* All the bounds are multiplied by $[m_{LQ}/(100 \text{ GeV})]^2$.

$(lq)(lq)$	h_{1L}	h_{1R}	h_{2L}	h_{2R}	h_{3L}	g_{1L}	g_{1R}	g_{2L}	g_{2R}	g_{3L}
(11)(13)	0.002	0.003		0.006	0.002	0.004		0.003	0.003	0.004
(21)(23)	0.0004	0.0004		0.0008	0.0004	0.004		0.0004	0.0004	0.0004

where the Mandelstam variables at the parton level are given by $\hat{s} = (p_{\bar{\nu}_e} + p_d)^2$, $\hat{t} = [p_{\bar{\nu}_e}(\text{initial}) - p_{\bar{\nu}_e}(\text{final})]^2$, and $\hat{u} = (p_{\bar{\nu}_e} - p_b)^2$.

In the u channel, two diagrams are mediated by the charge $= 1/3$, scalar LQs (S_1, S_3^0) with $T_3 = 0$ and one is mediated by a vector LQ ($V_{2\mu}^{-1/2}$) with $T_3 = -1/2$ [Fig. 2(b)]. The matrix element squared for all three diagrams contributing to the NC u -channel process is

$$\begin{aligned}
 & |\mathcal{M}_{LQ}^{u\text{-chann}}(\bar{\nu}_e d \rightarrow \bar{\nu}_e b)|^2 \\
 &= [\hat{u}(\hat{u} - m_b^2)] \left[\frac{|g_{1L}g_{1L}|^2}{(\hat{u} - M_{S_1}^2)^2} + \frac{|g_{3L}g_{3L}|^2}{(\hat{u} - M_{S_3^0}^2)^2} \right. \\
 & \left. + 2 \frac{|g_{1L}g_{3L}|^2}{(\hat{u} - M_{S_1}^2)(\hat{u} - M_{S_3^0}^2)} \right] + [4\hat{s}(\hat{s} - m_b^2)] \\
 & \times \left[\frac{|g_{2L}g_{2L}|^2}{(\hat{u} - M_{V_{2\mu}^{-1/2}}^2)^2} \right]. \tag{10}
 \end{aligned}$$

Having said all this about the relevant NC diagrams leading to b production, we now focus on the details that we use in order to compute the number of events for b/\bar{b} via the NC channel and demonstrate their behavior as a function of muon energy ranging from 0 to 250 GeV. We consider the contribution from LQs carrying different fermion numbers separately, which essentially means that *either all the h 's or all the g 's* contributing to a given process are nonzero at a time. For simplicity, we take the masses of scalar and vector LQs for both $F=0$ and $|F|=2$ to be equal ($= 250 \text{ GeV}$). As

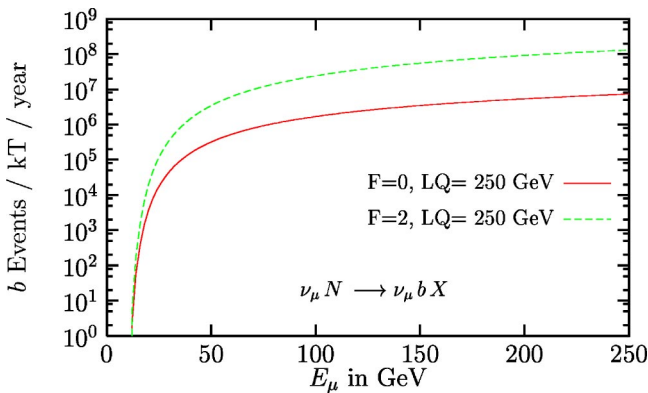


FIG. 3. Variation of b events (from LQ) for a 1 kT detector and LQ mass 250 GeV with muon beam energy for a baseline length 40 m and sample detector area 0.025 m².

in our earlier works [6,7], we have used CTEQ4LQ parton distribution functions [13] in order to compute the events. There is, however, significant suppression in phase space due to the production of the massive b quark. In our calculation we have not imposed any event selection cuts. Event selection cuts will further scale down the contribution (for a detailed analysis see Ref. [2]). We have considered a detector with a sample area of 0.025 m² [14] and placed at 40 m from the storage ring. Regarding the bounds on LQ couplings, we have used model independent constraints on the couplings to b quarks of B and L conserving LQs as discussed in [11], where it is shown that one can constrain the generation dependent LQ couplings to b quarks from the upper bounds on the flavor-changing decays $B \rightarrow l^+ l^- X$ (where $l^+ l^- = \mu^+ \mu^-, e^+ e^-$), the CKM matrix element V_{ub} , and from meson-antimeson ($B\bar{B}$) mixing, and obtain some of the best bounds for the processes of our interest. All the bounds on couplings that we have used for the calculation of event rates are listed in Table I. Since the bounds on the couplings h_{2L} and g_{1R} are not available from Ref. [11], we take them to be the same as bounds on couplings h_{2R} and g_{1L} (which are the opposite chirality counterparts of h_{2L} and g_{1R} , respectively). We make some simplifying assumptions, e.g., the product of couplings of different chiralities is obtained from the squares of the couplings of individual chiralities. We extract bounds relevant to the $(\nu_\mu d)(\nu_\mu b)$ vertex from the bounds for the (21)(23) generation of the quark-lepton pair, while for the vertex $(\bar{\nu}_e d)(\bar{\nu}_e b)$, we use the bounds for the (11)(13) generation indices relevant to the process. These bounds are derived from semileptonic inclusive B decays. The latest bounds coming from BABAR and BELLE experiments [15], however, are not relevant for the processes considered here except for the bound on V_{ub} , which does not make any significant change in the couplings. In Figs. 3 and 4, we have plotted the b -quark production rate as a function of muon beam energy for ν_μ - N and $\bar{\nu}_e$ - N scattering processes, respectively.

III. b (\bar{b}) PRODUCTION VIA CC PROCESSES

As discussed above, the production of \bar{b} or b in the final state through CC interaction can also occur in the SM at the tree level, in contrast to the NC case where SM contributes only at the one loop level. The SM cross sections for the CC processes $\nu_\mu + \bar{u} \rightarrow \mu^- + \bar{b}$ and $\bar{\nu}_e + u \rightarrow e^+ + b$ are given by

$$\begin{aligned}
 \frac{d^2\sigma}{dx dy}(\nu_\mu N \rightarrow \mu^- \bar{b} X) &= \frac{G_F^2 S}{\pi} \left(\frac{M_W^2}{M_W^2 + Q^2} \right)^2 \left(x' - x'y' \right. \\
 & \left. - \frac{m_b^2}{S} \right) (1 - y') \bar{u}(x') |V_{ub}|^2,
 \end{aligned}$$

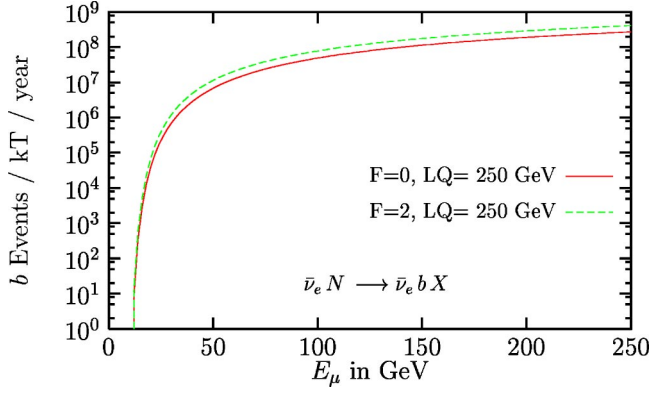


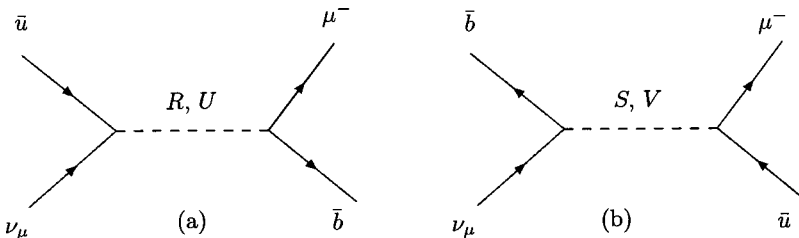
FIG. 4. Variation of b events (from LQ) for a 1 kT detector and LQ mass 250 GeV with muon beam energy for a baseline length 40 m and sample detector area 0.025 m^2 .

$$\frac{d^2\sigma}{dx dy}(\bar{\nu}_e N \rightarrow e^+ b X) = \frac{G_F^2 S}{\pi} \left(\frac{M_W^2}{M_W^2 + Q^2} \right)^2 \times \left(x' - x'y' - \frac{m_b^2}{S} \right) (1-y') u(x') |V_{ub}|^2. \quad (11)$$

Here we have the advantage of having the SM rates as benchmarks against which to compare the rates obtained via LQs. $\bar{u}(x')$ and $u(x')$ are the distribution functions of up-type antiquarks and quarks, respectively.

For the CC processes mentioned above, we can have both s - and u -channel diagrams arising from the relevant interaction terms in the effective LQ Lagrangian, as for the case of NC processes. For the first process, $\nu_\mu + \bar{u} \rightarrow \mu^- + \bar{b}$ (as shown in Fig. 3), there are four possible s -channel diagrams mediated by LQs (R^\dagger, U^\dagger) carrying $|F|=0$ and charge $= -2/3$. Also there are four possible u -channel diagrams that are mediated by LQs (S^\dagger, V^\dagger) carrying $|F|=2$ and charge $= -1/3$. For the second process, $\bar{\nu}_e + u \rightarrow e^+ + b$ (as shown in Fig. 4), the four possible s -channel diagrams are mediated by LQs (R, U) carrying $|F|=0$ and charge $= 2/3$, while the four possible u -channel diagrams are mediated by LQs (S, V) carrying $|F|=2$ and charge $= 1/3$, respectively. We first consider the production of \bar{b} from ν_μ (obtained from μ^- decay) through interactions with nucleons via the CC s -channel process for the $|F|=0$ case [Fig. 5(a)] and the CC u -channel process for the $|F|=2$ case [Fig. 5(b)].

There are, in all, four diagrams contributing to the production of \bar{b} via $\nu_\mu + \bar{u} \rightarrow \mu^- + \bar{b}$ in the s channel [Fig. 5(a)], one mediated by the charge $= -2/3$, scalar LQ ($R_2^{-1/2\dagger}$) with



$T_3 = -1/2$ and the other three by vector LQs ($U_{1\mu}^\dagger, U_{1\mu}^\dagger, U_{3\mu}^{0\dagger}$) with $T_3 = -1$. The matrix element squared for all four diagrams contributing to the CC s -channel process is

$$|\mathcal{M}_{LQ}^{s\text{-chann}}(\nu_\mu \bar{u} \rightarrow \mu^- \bar{b})|^2 = [\hat{s}(\hat{s} - m_b^2)] \left[\frac{|h_{2L} h_{2R}|^2}{(\hat{s} - M_{R_2^{-1/2}}^2)^2} + [4\hat{u}(\hat{u} - m_b^2)] \times \left[\frac{|h_{1L} h_{1L}|^2}{(\hat{s} - M_{U_{1\mu}}^2)^2} + \frac{|h_{3L} h_{3L}|^2}{(\hat{s} - M_{U_{3\mu}^0})^2} - 2 \frac{|h_{1L} h_{3L}|^2}{(\hat{s} - M_{U_{1\mu}}^2)(\hat{s} - M_{U_{3\mu}^0}^2)} \right] + [4(\hat{s} + \hat{u})(\hat{s} + \hat{u} - m_b^2)] \left[\frac{|h_{1L} h_{1R}|^2}{(\hat{s} - M_{U_{1\mu}}^2)^2} \right], \quad (12)$$

where the Mandelstam variables at the parton level are given by $\hat{s} = (p_{\nu_\mu} + p_{\bar{u}})^2$, $\hat{t} = (p_{\nu_\mu} - p_{\mu^-})^2$, and $\hat{u} = (p_{\nu_\mu} - p_{\bar{b}})^2$.

In the u channel, three diagrams are mediated by the charge $= -1/3$, scalar LQs ($S_1^\dagger, S_1^\dagger, S_3^{0\dagger}$) with $T_3 = 0$ and one is mediated by a vector LQ ($V_{2\mu}^{-1/2\dagger}$) with $T_3 = -1/2$ [Fig. 5(b)]. The matrix element squared for all four diagrams contributing to the CC u -channel process is

$$|\mathcal{M}_{LQ}^{u\text{-chann}}(\nu_\mu \bar{u} \rightarrow \mu^- \bar{b})|^2 = [\hat{u}(\hat{u} - m_b^2)] \left[\frac{|g_{1L} g_{1L}|^2}{(\hat{u} - M_{S_1}^2)^2} + \frac{|g_{1L} g_{1R}|^2}{(\hat{u} - M_{S_1}^2)^2} + \frac{|g_{3L} g_{3L}|^2}{(\hat{u} - M_{S_3^0}^2)^2} - 2 \frac{|g_{1L} g_{3L}|^2}{(\hat{u} - M_{S_1}^2)(\hat{u} - M_{S_3^0}^2)} \right] + [4(\hat{s} + \hat{u}) \times (\hat{s} + \hat{u} - m_b^2)] \left[\frac{|g_{2L} g_{2L}|^2}{(\hat{u} - M_{V_{2\mu}^{-1/2}}^2)^2} \right]. \quad (13)$$

Next we consider the production of b from $\bar{\nu}_e$ (also obtained from the μ^- decay) through interactions with nucleons via the CC s -channel process for the $|F|=0$ case [Fig. 6(a)] and the CC u -channel process for the $|F|=2$ case [Fig. 6(b)]. There are, in all, four diagrams contributing to the

FIG. 5. b production via CC process ($\nu_\mu + \bar{u} \rightarrow \mu^- + \bar{b}$) from scalar and vector LQs: (a) s -channel diagram corresponding to $|F|=0$ LQs and (b) u -channel diagram corresponding to $|F|=2$ LQs.

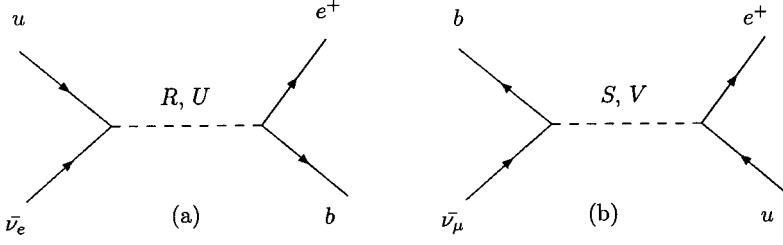


FIG. 6. b production via CC process ($\bar{\nu}_e + u \rightarrow e^+ + b$) from scalar and vector LQs: (a) s -channel diagram corresponding to $|F|=0$ LQs and (b) u -channel diagram corresponding to $|F|=2$ LQs.

production of b via $\bar{\nu}_e + u \rightarrow e^+ + b$ in the s channel [Fig. 6(a)], one mediated by the charge = 2/3, scalar LQ ($R_2^{-1/2}$) with $T_3 = -1/2$, while the other three are mediated by vector LQs ($U_{1\mu}, U_{1\mu}, U_{3\mu}^0$) having $T_3=0$ each. The matrix element squared for the four diagrams contributing to the CC s -channel process is

$$\begin{aligned}
 |\mathcal{M}_{LQ}^{s\text{-chann}}(\bar{\nu}_e u \rightarrow e^+ b)|^2 &= [\hat{s}(\hat{s} - m_b^2)] \left[\frac{|h_{2L}h_{2R}|^2}{(\hat{s} - M_{R_2^{-1/2}}^2)^2} \right] + [4\hat{u}(\hat{u} - m_b^2)] \\
 &\times \left[\frac{|h_{1L}h_{1L}|^2}{(\hat{s} - M_{U_{1\mu}}^2)^2} + \frac{|h_{3L}h_{3L}|^2}{(\hat{s} - M_{U_{3\mu}^0}^2)^2} \right. \\
 &\left. - 2 \frac{|h_{1L}h_{3L}|^2}{(\hat{s} - M_{U_{1\mu}}^2)(\hat{s} - M_{U_{3\mu}^0}^2)} \right] + [4(\hat{s} + \hat{u})(\hat{s} + \hat{u} - m_b^2)] \\
 &\times \left[\frac{|h_{1L}h_{1R}|^2}{(\hat{s} - M_{U_{1\mu}}^2)^2} \right] \quad (14)
 \end{aligned}$$

where the Mandelstam variables at the parton level are given by $\hat{s} = (p_{\bar{\nu}_e} + p_u)^2$, $\hat{t} = (p_{\bar{\nu}_e} - p_{e^+})^2$, and $\hat{u} = (p_{\bar{\nu}_e} - p_b)^2$.

In the u channel, three diagrams are mediated by the charge = 1/3, scalar LQs (S_1, S_1, S_3^0) with $T_3=0$ and one is mediated by a vector LQ ($V_{2\mu}^{-1/2}$) with $T_3 = -1/2$ [Fig. 6(b)]. The matrix element squared for all four diagrams contributing to the CC u -channel process is

$$\begin{aligned}
 |\mathcal{M}_{LQ}^{u\text{-chann}}(\bar{\nu}_e u \rightarrow e^+ b)|^2 &= [\hat{u}(\hat{u} - m_b^2)] \left[\frac{|g_{1L}g_{1L}|^2}{(\hat{u} - M_{S_1}^2)^2} + \frac{|g_{1L}g_{1R}|^2}{(\hat{u} - M_{S_1}^2)^2} + \frac{|g_{3L}g_{3L}|^2}{(\hat{u} - M_{S_3^0}^2)^2} \right. \\
 &\left. - 2 \frac{|g_{1L}g_{3L}|^2}{(\hat{u} - M_{S_1}^2)(\hat{u} - M_{S_3^0}^2)} \right] + [4(\hat{s} + \hat{u})(\hat{s} + \hat{u} - m_b^2)] \\
 &\times \left[\frac{|g_{2L}g_{2L}|^2}{(\hat{u} - M_{V_{2\mu}^{-1/2}}^2)^2} \right]. \quad (15)
 \end{aligned}$$

As discussed in the previous section, we have used the model independent bounds on couplings from [11], and the relevant bounds for the processes given above are listed in Table I. We extract bounds relevant to the $(\nu_\mu \bar{u})(\mu^- \bar{b})$ vertex from the bounds for the (21)(23) generation of the quark-lepton pair, while for the vertex $(\bar{\nu}_e u)(e^+ b)$, we use the bounds for the (11)(13) generation indices relevant for the process $\bar{\nu}_e u \rightarrow e^+ b$. The other inputs to compute the event rates are the same as for the NC diagrams. In Figs. 7 and 8, we have plotted the \bar{b} and b event rates as functions of muon beam energy for ν_μ - N and $\bar{\nu}_e$ - N scattering processes, respectively. For these processes we have also plotted the SM contribution to \bar{b} and b events. To determine the allowed range of LQ masses and products of couplings, we have used the criterion that the number of signal events is equal to two or five times the square root of events in the SM. Accepting this requirement of the 2σ and 5σ effect as a sensible discovery criterion, the contours in Figs. 9 and 10 are drawn for a baseline length of 40 m and thus the noncompliance of these

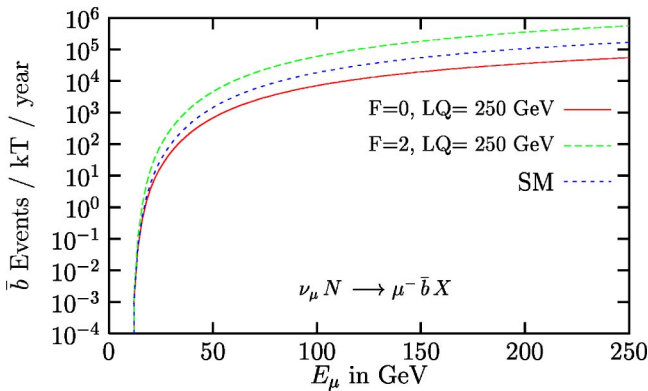


FIG. 7. Variation of \bar{b} events (from SM and LQ) for a 1 kT detector and LQ mass 250 GeV with muon beam energy for a baseline length 40 m and sample detector area 0.025 m².

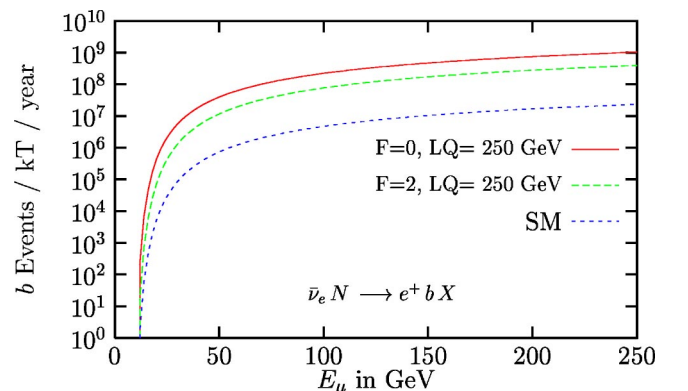


FIG. 8. Variation of b events (from SM and LQ) for a 1 kT detector and LQ mass 250 GeV with muon beam energy for a baseline length 40 m and sample detector area 0.025 m².

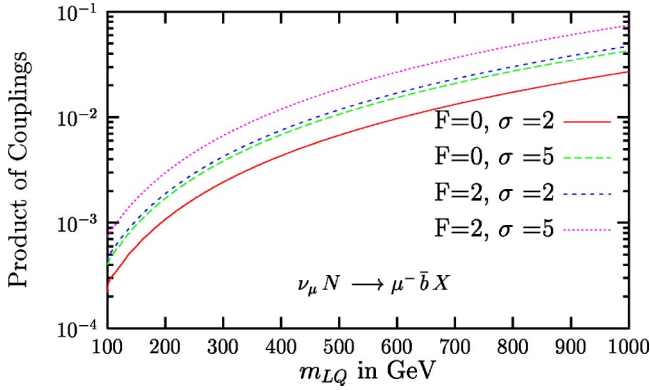


FIG. 9. Contour plot for \bar{b} production at 2σ and 5σ effect for $E_\mu = 50$ GeV, baseline length = 40 m and sample detector of area 2500 cm^2 and mass 1 kT.

estimates with experimental observation would mean that the region above these curves is ruled out.

IV. CONCLUSIONS AND DISCUSSION

Heavy quark (b, \bar{b}) production from ν_μ - N and $\bar{\nu}_e$ - N scattering via both the CC and NC interactions at a NF provides an exciting possibility of detecting signals of new physics. This comes about because in these processes the SM contribution is heavily suppressed either due to the CKM matrix element or due to the interaction of neutrinos with the sea quarks present inside the nucleon. The NC processes in SM are further suppressed as they can take place only at one loop level. We have computed here the b (\bar{b}) event rates in theories with LQ and confined ourselves to the near-site experiments where the oscillation effects are negligible. From Fig. 7, it is clear that the contribution coming from the SM to the \bar{b} production rate in the CC channel is higher than that of LQs with $|F|=0$, while it is lower than the contribution from LQs with $|F|=2$ for our choice of the couplings obtained from low energy experiments. We typically find (Fig.

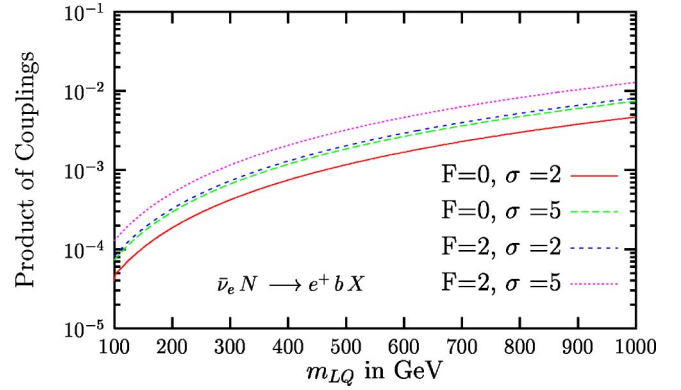


FIG. 10. Contour plot for b production at 2σ and 5σ effect for $E_\mu = 50$ GeV, baseline length = 40 m and sample detector of area 2500 cm^2 and mass 1 kT.

8) that the SM contribution to the b production rate is two to three orders of magnitude smaller than the LQ contribution in the CC channel, even after using the most severe constraints on LQ couplings and masses from low energy FCNC processes. Further the b production rate in the NC channel (Figs. 3 and 4) is comparable to that for the CC case. We have investigated the region in the coupling-mass space for LQs, which can provide a reasonable signal for the discovery of new physics involving LQs. It may be noted that this region can be even more restrictive than that implied by the low energy bounds obtained from B meson decays. Also the inclusion of LFV interactions via LQ's could further squeeze the allowed region of LFV couplings and masses.

ACKNOWLEDGMENTS

P.M. acknowledges the Council for Scientific and Industrial Research, India, while A.G. acknowledges the University Grants Commission, India for partial financial support. We also acknowledge SERC, Department of Science & Technology, New Delhi, for partial financial support.

[1] S. Dutta, R. Gandhi, and B. Mukhopadhyaya, *Eur. Phys. J. C* **18**, 405 (2000); C. Quigg, hep-ph/9803326; S. Geer, *Phys. Rev. D* **57**, 6989 (1998); D. Ayres *et al.*, physics/9911009; A. Cervera *et al.*, *Nucl. Phys.* **B593**, 73(E) (2001); A. Blondel *et al.*, Report No. CERN-EP-2000-05; C. Albright *et al.*, hep-ex/0008064; S. Geer, *Comments Nucl. Part. Phys.* **42**, 284 (2002).
[2] M.L. Mangano *et al.*, hep-ph/0105155.
[3] Y. Fukuda *et al.*, *Phys. Lett. B* **433**, 9 (1998); *Phys. Rev. Lett.* **81**, 1562 (1998); T. Kagita, in Proceedings of the XVIIIth International Conference on Neutrino Physics and Astrophysics, Takayama, Japan, 1998.
[4] L. Wolfenstein, *Phys. Rev. D* **17**, 2369 (1978); **20**, 2634 (1979); S.P. Mikheyev and A. Yu Smirnov, *Sov. J. Nucl. Phys.* **42**, 913 (1986).
[5] B. Pontecorvo, *Sov. Phys. JETP* **26**, 984 (1968).

[6] A. Datta, R. Gandhi, B. Mukhopadhyaya, and P. Mehta, *Phys. Rev. D* **64**, 015011 (2001).
[7] P. Mehta, A. Goyal, and S. Dutta, *Phys. Lett. B* **535**, 219 (2002).
[8] D. Chakraverty, A. Dutta, and B. Mukhopadhyaya, *Phys. Lett. B* **503**, 74 (2001).
[9] J.C. Pati and Abdus Salam, *Phys. Rev. D* **10**, 275 (1974); O. Shankar, *Nucl. Phys.* **B206**, 253 (1982); W. Buchmuller and D. Wyler, *Phys. Lett. B* **177**, 377 (1986); W. Buchmuller, R. Ruckl, and D. Wyler, *ibid.* **191**, 442 (1987); P. Langacker, M. Luo, and Alfred K. Mann, *Rev. Mod. Phys.* **64**, 87 (1992); J. Blumlein and R. Ruckl, *Phys. Lett. B* **304**, 337 (1993); M.A. Doncheski and R.W. Robinett, *Phys. Rev. D* **56**, 7412 (1997); U. Mahanta, *ibid.* **62**, 073009 (2000).
[10] See the third and sixth references in [9].
[11] S. Davidson, D. Bailey, and B.A. Campbell, *Z. Phys. C* **61**,

- 613 (1994); E. Gabrielli, Phys. Rev. D **62**, 055009 (2000).
- [12] S. Aid *et al.*, Phys. Lett. B **353**, 578 (1995); Derrick *et al.*, Z. Phys. C **73**, 613 (1997); C. Adloff *et al.*, hep-ex/9907002.
- [13] H. Lai *et al.*, Phys. Rev. D **55**, 1280 (1997).
- [14] C. Albright *et al.* [1].
- [15] Belle Collaboration, K. Abe *et al.*, hep-ex/0204002; BABAR Collaboration, B. Aubert *et al.*, hep-ex/0207080; A. Roodman, hep-ex/0112019; V. Halyo, hep-ex/0207010; Belle Collaboration, J. Nam *et al.*, Int. J. Mod. Phys. A **16**, Proc. Suppl. 1B 625 (2001).